Report Documentation Page

Form Approved
OMB No. 0704-0188

1. REPORT DATE	2. REPORT TYPE	3. DATES COVERED
JUN 2014		**00-00-2014 to 00-00-2014**

4. TITLE AND SUBTITLE	5a. CONTRACT NUMBER
Physics-based Stabilization of Spectral Elements for the 3D Euler Equations of Moist Atmospheric Convection	5b. GRANT NUMBER
	5c. PROGRAM ELEMENT NUMBER
6. AUTHOR(S)	5d. PROJECT NUMBER
	5e. TASK NUMBER
	5f. WORK UNIT NUMBER
7. PERFORMING ORGANIZATION NAME(S) AND ADDRESS(ES) **Naval Postgraduate School,Department of Applied Mathematics,Monterey,CA,93943**	8. PERFORMING ORGANIZATION REPORT NUMBER
9. SPONSORING/MONITORING AGENCY NAME(S) AND ADDRESS(ES)	10. SPONSOR/MONITOR'S ACRONYM(S)
	11. SPONSOR/MONITOR'S REPORT NUMBER(S)

12. DISTRIBUTION/AVAILABILITY STATEMENT
Approved for public release; distribution unlimited

13. SUPPLEMENTARY NOTES

14. ABSTRACT

15. SUBJECT TERMS

16. SECURITY CLASSIFICATION OF:			17. LIMITATION OF ABSTRACT	18. NUMBER OF PAGES	19a. NAME OF RESPONSIBLE PERSON
a. REPORT	b. ABSTRACT	c. THIS PAGE			
unclassified	**unclassified**	**unclassified**	**Same as Report (SAR)**	**9**	

PHYSICS-BASED STABILIZATION OF SPECTRAL ELEMENTS FOR THE 3D EULER EQUATIONS OF MOIST ATMOSPHERIC CONVECTION

SIMONE MARRAS, ANDREAS MÜLLER, FRANCIS X. GIRALDO

Dept. Appl. Mathematics, Naval Postgraduate School, Monterey, CA, USA.
email: {smarras1,amueller,fxgirald}@nps.edu

In the context of stabilization of high order spectral elements, we introduce a dissipative scheme based on the solution of the compressible Euler equations that are regularized through the addition of a residual-based stress tensor. Because this stress tensor is proportional to the residual of the unperturbed equations, its effect is close to none where the solution is sufficiently smooth, whereas it increases elsewhere. This paper represents a first extension of the work by Nazarov and Hoffman [Nazarov M. and Hoffman J. (2013), *Int. J. Numer. Methods Fluids, 71:339-357.*] to high-order spectral elements in the context of low Mach number atmospheric dynamics. The simulations show that the method is reliable and robust for problems with important stratification and thermal processes such as the case of moist convection. The results are partially compared against a Smagorinsky solution. With this work we mean to make a step forward in the implementation of a stabilized, high order, spectral element large eddy simulation (LES) model within the Nonhydrostatic Unified Model of the Atmosphere, NUMA.

1 Introduction

Recently [17], a numerically stable and computationally inexpensive large-eddy simulation (LES) model for compressible flows was designed for adaptive finite elements. It is a close relative of the entropy-viscosity method by Guermond and co-workers (see, e.g. [7]), although no entropy equation is used to construct the dynamic viscosity coefficient of the stress tensor.

In the current paper, we explore the capabilities of the aforementioned LES model to act as a stabilization method for the spectral element solution of the Euler equations at the low Mach number regimes typical of atmospheric flows. This effort is justified by the fact that, within the community of atmospheric modelers, there is still a widespread concern about the most proper stabilization scheme to be used with either Galerkin or other approximation methods of the equations of atmospheric dynamics. Although the use of residual-based stabilizing schemes has been largely assessed for the finite element method during the past thirty years (e.g. Streamline-Upwind/Petrov-Galerkin (SUPG) [3], Galerkin/Least-Squares (GLS) [10], Variational Multiscale (VMS) [9, 8, 2, 14]), hyper viscosity is still today the most classical approach in spite of its important drawbacks and mathematical inconsistency.

This work is a first step toward the implementation of a stabilized high order spectral element LES model (LES-SEM) for the *Nonhydrostatic Unified Model of the Atmosphere* (NUMA) developed by the authors [11, 5]. The rest of the paper is organized as follows. The set of equations and the LES model are described in Section 2. Some basics on the space and time discretization of these equations is reported in Section 3, which is followed by the numerical tests and results in Section 4. Some conclusions are given in Section 5.

2 Equations for wet dynamics

Let $\Omega \in \mathbb{R}^3$ be a fixed three dimensional domain with boundary $\partial\Omega$ and Cartesian coordinates $\mathbf{x} = (x, y, z)$. Let us identify the dry air density, the velocity vector, and the potential temperature with the symbols $\rho, \mathbf{u}$, and θ. Let us also define the mixing ratios of water vapor, cloud water, and rain as $q_v = \rho_v/\rho, q_c = \rho_c/\rho$ and $q_r = \rho_r/\rho$, where $\rho_{v,c,r}$ are the densities of vapor, cloud, and rain. Furthermore, let $\rho'(t, \mathbf{x}) = \rho(t, \mathbf{x}) - \rho_0(z)$, $\theta'(t, \mathbf{x}) = \theta(t, \mathbf{x}) - \theta_0(z)$, and $p'(t, \mathbf{x}) = p(t, \mathbf{x}) - p_0(z)$ be the perturbations of density, potential temperature, and pressure with respect to a hydrostatically balanced background state indicated by the subscript *0*. Then, the strong form of the time-dependent Euler equations with gravity, g, can be written as:

$$\begin{aligned} \rho'_t + \mathbf{u} \cdot \nabla\rho + \rho\nabla \cdot \mathbf{u} &= 0, \\ \mathbf{u}_t + \mathbf{u} \cdot \nabla\mathbf{u} + \tfrac{1}{\rho}\nabla \cdot (\mathbf{I}p') &= g(1 + \epsilon q_v - q_c - q_r)\mathbf{k}, \\ \theta'_t + \mathbf{u} \cdot \nabla\theta &= S_\theta(\rho, \theta, q_v, q_c, q_r), \\ q_{i_t} + \mathbf{u} \cdot \nabla q_i &= S_{q_i}(\rho, \theta, q_v, q_c, q_r), \qquad \text{for } i = v, c, r, \end{aligned} \tag{1}$$

where $\mathbf{I}$ is the identity matrix, $\mathbf{k}$ is the unit vector $[0\,0\,1]^{\mathcal{T}}$, and $\epsilon = R/R_v$ is the ratio of the gas constant of dry air, R and the constant of water vapor, R_v. Because moist air contributes to the buoyancy of the flow, the right hand side of the momentum equation is corrected with total buoyancy $\mathbf{B} = g(1 + \epsilon q_v - q_c - q_r)\mathbf{k}$. Due to the microphysical processes that involve phase change in the water content, the source/sink term S at the right-hand side of the equations of potential temperature and water tracers must be computed. These processes are modeled by the Kessler parameterization [12]. Equations (1) must be solved in Ω $\forall t \in (0, T)$. Initial and boundary conditions will be assigned. θ, ρ, and p are related through the equation of state for a perfect gas.

2.1 Dynamic dissipation in an LES sense

The boundedness of the solution computed with the straightforward SEM approximation of (1) is compromised by unphysical Gibbs oscillations. To stabilize the problem, the Euler equations are corrected to include the stresses of the Navier-Stokes equations, where, however, the viscosity coefficients of such stresses are given by a residual-based approximation that leads the problem to converge to the entropy solution, as proved in [16].

Remark 1 Because a saturation adjustment scheme [19] is used to treat the moist thermodynamics, the source terms are set to zero in the main step of the solution, and are only computed within the Kessler sub-step. For this reason, the sources will not appear in the regularized version of Equations (1).

We write:

$$
\begin{aligned}
\rho'_t + \mathbf{u}\cdot\nabla\rho + \rho\nabla\cdot\mathbf{u} &= \nabla\cdot(\nu_n\nabla\rho) \\
\mathbf{u}_t + \mathbf{u}\cdot\nabla\mathbf{u} + \tfrac{1}{\rho}\nabla\cdot(\mathbf{I}p) &= \tfrac{1}{\rho}\nabla\cdot\left(\mu_n\left(\nabla\mathbf{u} + \nabla\mathbf{u}^{\mathrm{T}}\right)\right) + \mathbf{B} \\
\theta_t + \mathbf{u}\cdot\nabla\theta &= \nabla\cdot(\kappa_n\nabla\theta) \\
q_{i_t} + \mathbf{u}\cdot\nabla q_i &= \nabla\cdot(\nu_c\nabla\theta)\,.
\end{aligned}
\tag{2}
$$

Except for ν_c that, for the time being, is set to a constant, the viscosity coefficients that appear in the first five equations are computed dynamically as a function of the solution. They are calculated element-wise on every high order element Ω_e. More specifically, given the sensible temperature $T = \theta(p/p_0)^{R/c_p}$ and one element with equivalent length $\bar{h}_{\Omega_e}$, we start by defining the dynamic viscosities

$$
\mu_{\max}|_{\Omega_e} = 0.5\bar{h}_{\Omega_e}\,\|\rho^n\|_{\infty,\Omega_e}\,\||\mathbf{u}^n| + \sqrt{\gamma T^n}\|_{\infty,\Omega_e}, \tag{3}
$$

and

$$
\mu_1|_{\Omega_e} = \bar{h}^2_{\Omega_e}\max\left(\|\rho^n\|_{\infty,\Omega}\,\frac{\|R(\rho)\|_{\infty,\Omega_e}}{\|\rho^n - \bar{\rho}^n\|_{\infty,\Omega}}, \frac{\|R(\mathbf{u})\|_{\infty,\Omega_e}}{\|\mathbf{u}^n - \bar{\mathbf{u}}^n\|_{\infty,\Omega}}, \frac{\|R(\theta)\|_{\infty,\Omega_e}}{\|\theta^n - \bar{\theta}^n\|_{\infty,\Omega}}\right), \tag{4}
$$

where $\bar{\cdot}$ indicates the space average of the quantity at hand over Ω and the $\|\cdot\|_{\infty,\Omega}$ terms at the denominator are used for normalization for a consistent dimension of the resulting equation. Having $\mu_{\max}$ and μ_1 constructed, we can compute the dynamics coefficients of the viscosity terms in Equations (2) as:

$$
\mu_n|_{\Omega_e} = \min\left(\mu_{\max}|_{\Omega_e}, \mu_1|_{\Omega_e}\right), \quad \kappa_n|_{\Omega_e} = \frac{\mathrm{Pr}}{\gamma - 1}\mu_n|_{\Omega_e}, \quad \nu_n|_{\Omega_e} = \frac{\mathrm{Pr}}{\|\rho^n\|_{\infty,\Omega_e}}\mu_n|_{\Omega_e}, \tag{5}
$$

where $Pr = 0.7$ is the Prandtl number of dry air.

Remark 2 To keep the discussion brief, the details of the derivation of the equations is not reported and the notation is somewhat abused. A proper formulation will be reported in a subsequent paper.

3 Space and time discretization

Equations (2) are approximated in space by high order spectral elements and by an Implicit-Explicit (IMEX) method in time. Details can be found in, e.g. [6] (SEM) and [5] (IMEX).

4 Numerical Tests

The SEM-LES method is tested against benchmarks of ubiquitous use when testing new atmospheric dynamical cores. First, the model is verified in dry mode. We perturb a neutrally stable atmosphere with a cold thermal anomaly that triggers the development of a density current. Once we have verified the ability of the model to handle dry dynamics, we solve a fully three-dimensional supercell triggered by the thermal perturbation of a realistic, moist, partially unstable background state.

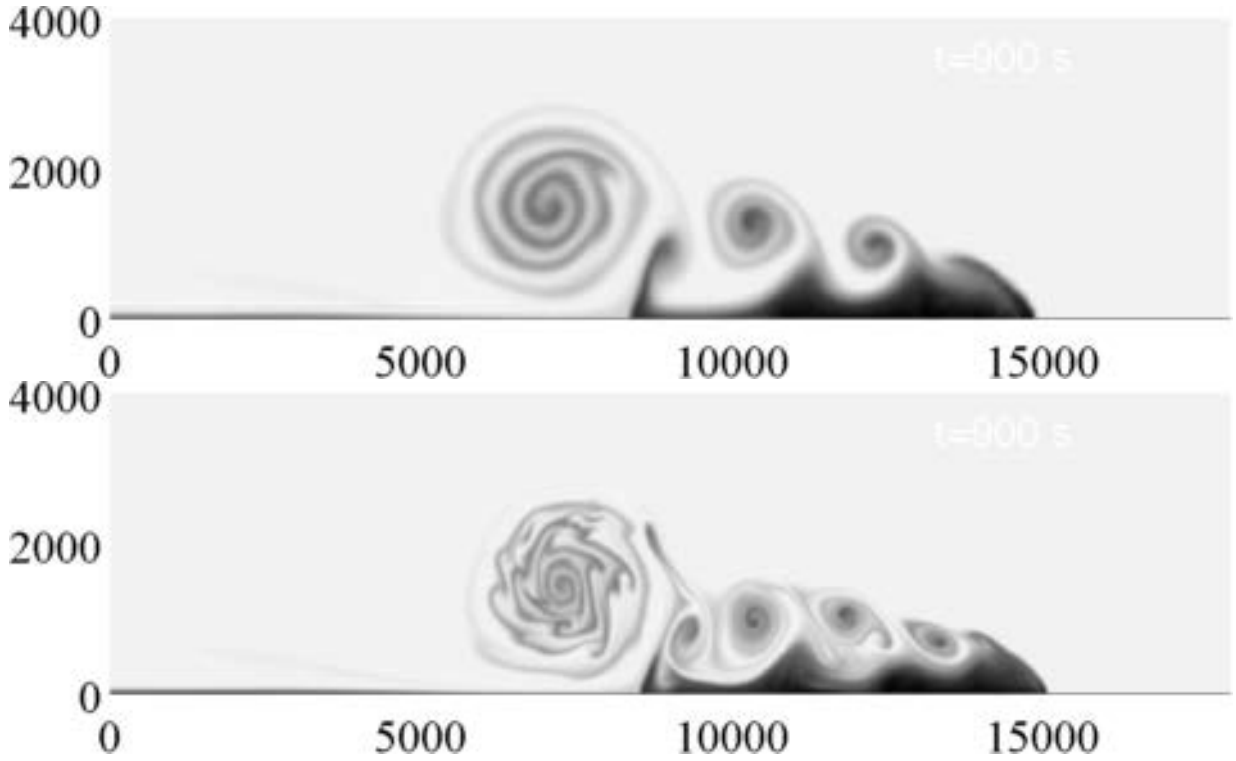

Figure 1: Density current: θ' at 900 s. Top: $128 \times 1 \times 32$ el. ($\overline{\Delta z} = \overline{\Delta x} \approx 50$ m). Bottom: $256 \times 1 \times 64$ el. ($\overline{\Delta z} = \overline{\Delta x} \approx 25$ m). 4^{th}-order elements.

4.1 Density current in a pseudo-3D domain

The density current is a standard benchmark in the development of atmospheric codes [20]. The inviscid version of [1] is used for our analysis. This is because we are interested in assessing the current LES-like approach as a stabilizing tool that does not require further viscosity. The background state is characterized by a neutral atmosphere at uniform potential temperature $\theta = 300$ K and hydrostatically balanced pressure. Due to the symmetry of the original problem with respect to the plane center line of the $x - z$ plane, the solution is computed in the region $\Omega = 25.6 \times \infty \times 6.4\,\mathrm{km}^3$ The perturbation θ' centered in $(x_c, z_c) = (0, 3)\,\mathrm{km}$ has radii $(r_x, r_y, r_z) = (4, \infty, 2)\,\mathrm{km}$ and is given by $\theta' = 0.5\Delta\theta\,(1 + \cos(\pi_c R))$ for $R \leq 1$, with amplitude $\Delta\theta = -15$ K and section $R = \sqrt{(x - x_c)/r_x^2 + (z - z_c)/r_z^2}$. Periodic boundary conditions are used along y whereas no-flux conditions are set in x and z. The initial velocity is zero everywhere. Figure 1 shows the fully developed current at time $t = 900\,\mathrm{s}$ on two grids with uniform resolutions $\Delta x = \Delta z = 50\,m$ and $\Delta x = \Delta z = 25\,m$. To measure the front position at $t_f = 900\,\mathrm{s}$, we take the node on the ground where $\theta' = -1$ K. A comparison of the front position and $\theta'_{max,min}$ with respect to previous work is reported in Table 1. As the resolution decreases, the front appears slower; this fact is also observed in Fig. 5 of [20].

We are aiming at using the current stabilizing scheme as a Large Eddy Simulation scheme. As a first analysis in this direction, we compare how the current model compares with the classical model by Lilly and Smagorinsky [13, 18]. The Smagorinsky solution (implemented within NUMA as well) is plotted in Figure 2. A more thorough and quantitative analysis is currently being carried out by the authors. At a resolution $\overline{\Delta z} = \overline{\Delta x} \approx 25$m and by plotting comparable contours (values not shown in the plot), the two models are highly comparable, although the degree of dissipation of the current scheme seems lower than Smagorinsky's using a Smagorinsky constant $C_s = 0.14$.

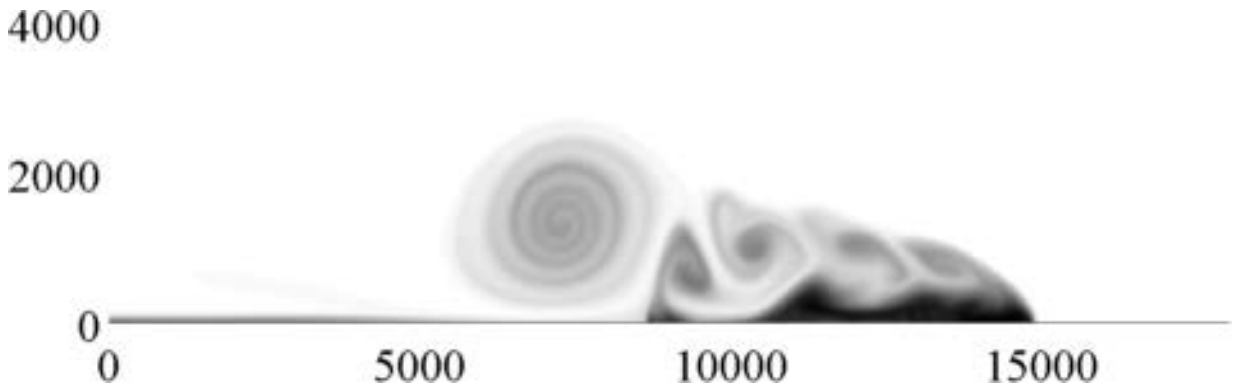

Figure 2: Density current using a classical Smagorinsky SGS scheme with constant $C_s = 0.14$: θ' at $900s$. $256 \times 1 \times 64$ el. ($\overline{\Delta z} = \overline{\Delta x} \approx 25$m). 4^{th}-order elements.

Significantly more sub-grid structures are resolved using the current model. Further analysis is though required.

Remark 3 Throughout this paper we have discussed an LES approach to stabilization. Nevertheless, it must be pointed out that the simulations that we have presented are not necessarily to be viewed as LES simulations unless finer grids are used.

4.2 3D moist convection

The three-dimensional simulation of a convective cell is defined in the domain $160 \times 120 \times 24\,\mathrm{km}^3$. The initial field is perturbed by a temperature anomaly θ' 3 K warmer than the surrounding environment, which is given by the sounding of [4]. The domain Ω^h is subdivided into $40 \times 30 \times 24$ elements of order 4. A stretched grid along z is used to make the resolution higher in the lower atmosphere where convection is triggered. The domain is crossed by a horizontal wind along the x-direction with a $12\,\mathrm{m\,s}^{-1}$ shear at $z = 2000\,\mathrm{m}$. A no-slip condition is applied on the surface boundary while periodic boundaries are defined along x and y. A Rayleigh type absorbing layer is included at $z \geq 19000\,\mathrm{m}$. The cloud first forms at approximately 500 s, and is fully develop after 4500 s. A 3D instantaneous view of q_c is plotted in Figure 3. Qualitatively, it is comparable to previous results on a similar case. A quantitative evaluation of the instantaneous rain on the ground is plotted in Figure 4a, whereas the cloud content obtained by averaging q_c along the $y-$direction is plotted in Figure 4b.

5 Conclusions

We extended to high order spectral elements the LES-based stabilization method first introduced in [17] for the finite element solution of fully compressible flows. We explored the capabilities of this inexpensive technique to solve the Euler equations of stratified flows at the low-Mach regimes encountered in atmospheric flows. When applied to dry and moist simulations, the current implementation appears to give satisfactory results that are comparable to others presented in the literature. Without the need for any additional viscosity, this dynamic LES scheme proved to be sufficient to stabilize the spectral element solution of the Euler equations in atmospheric applications. However, since a thorough analysis was not carried out to evaluate this approach in terms

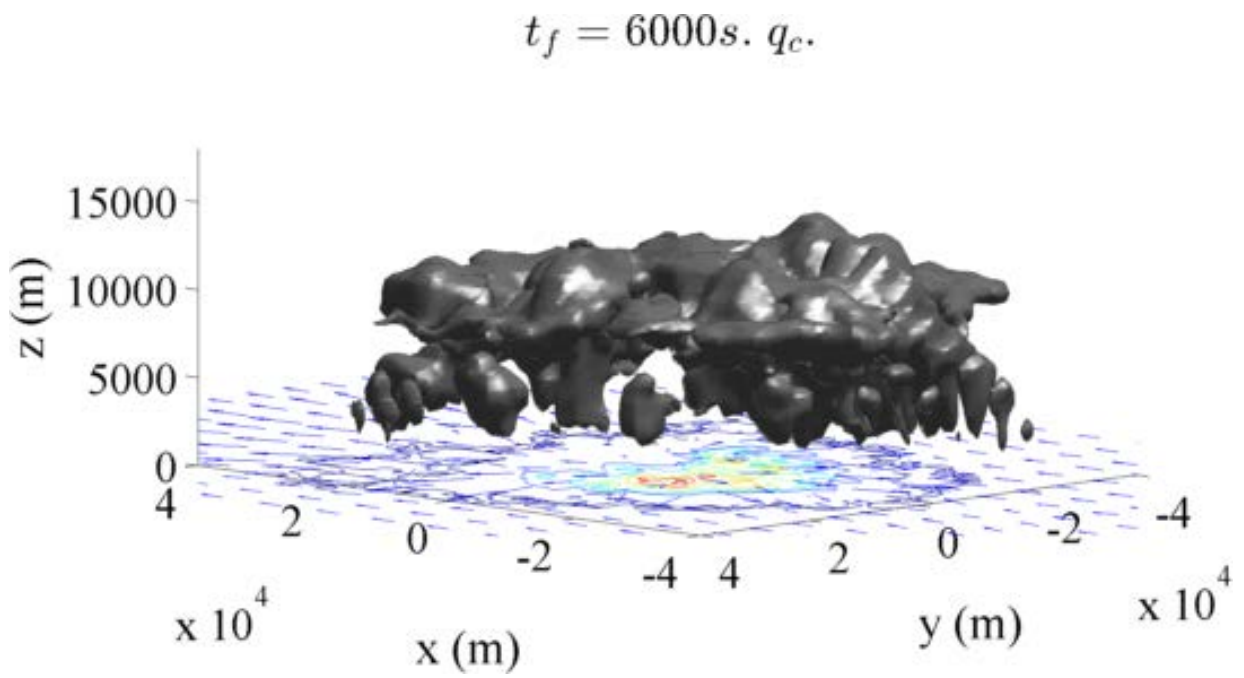

Figure 3: Supercell: 3d view (using az = -135 and el = 8) of q_c (grey surface), surface velocity (vectors), and the instantaneous distribution of q_r on the ground (contours).

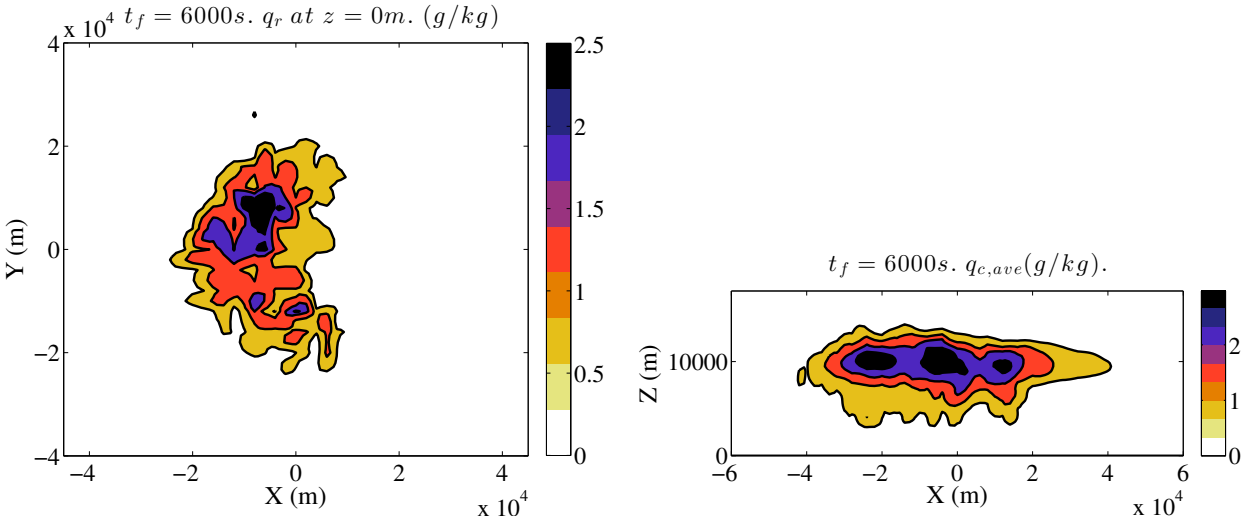

(a) Instantaneous rain distribution on the ground at $t = 6000$ s.

(b) Vertical slice of the distribution of q_c averaged along the y direction.

Figure 4: 3D supercell: horizontal slice of q_r at $z = 0$ m and y-averaged q_c at $t = 6000$ s.

Table 1: Case 3. Comparative results of front location at 900s. LES (SEM), VMS (FE), WRF-ARW V2.2 (FD), f-wave (FV), filtered Spectral Elements (SE), filtered Discontinuous Galerkin (DG), REFC, REFQ and PPM results are compared. All models but LES and VMS used artificial diffusion with constant $\mu = 75\,\mathrm{m}^2\,\mathrm{s}^{-1}$.

Model	N_{el}	Order	$\mu = 75\,\mathrm{m}^2\,\mathrm{s}^{-1}$	Front Location [m]
LES (25 m)	$256 \times 1 \times 64$	4^{th}	NO	15080
LES (50 m)	$128 \times 1 \times 32$	4^{th}	NO	14888
LES (100 m)	$64 \times 1 \times 16$	4^{th}	NO	14546
LES (200 m)	$32 \times 1 \times 8$	4^{th}	NO	13736
LES	$32 \times 1 \times 8$	6^{th}	NO	14568
LES	$32 \times 1 \times 8$	8^{th}	NO	14754
VMS [15] (25 m)			NO	14890
VMS [15] (50 m)			NO	14629
VMS [15] (75 m)			NO	14487
VMS [15] (100 m)			NO	14355
WRF-ARW 50 m			YES	14470
SE [6] 50m			YES	14767
DG [6] 50m			YES	14767
f-wave (FV) [1] 50 m			YES	14975
REFC [20] 50 m			YES	14437
PPM [20] 50 m			YES	15027

of its turbulence modeling properties, much additional work is necessary to fully assess it in its applicability as a turbulence closure for atmospheric simulations.

6 Acknowledgements

The authors are thankful to Dr. Murtazo Nazarov for his clarifications about the original method. They also gratefully acknowledge the support of the Office of Naval Research through program element PE-0602435N, the National Science Foundation (Division of Mathematical Sciences) through program element 121670, and the Air Force Office of Scientific Research through the Computational Mathematics program. The first and second authors were supported by the National Academies through a National Research Council fellowship.

REFERENCES

[1] N. Ahmad and J. Lindeman. Euler solutions using flux-based wave decomposition. *Int. J. Numer. Meth. Fluids*, 54:47–72, 2007.

[2] M. Avila, R. Codina, and J. Principe. Large eddy simulation of low mach number flows using dynamic and orthogonal subgrid scales. *Comput. Fluids*, 99:44–66, 2014.

[3] A N Brooks and T J R Hughes. Streamline upwind/Petrov-Galerkin formulations for convective dominated flows with particular emphasis on the incompressible navier-stokes equations. *Comput. Methods Appl. Mech. Eng.*, 32:199–259, 1982.

[4] S. Gaberšek, F. X. Giraldo, and J. Doyle. Dry and moist idealized experiments with a two-dimensional spectral element model. *Mon. Wea. Rev.*, 140:3163–3182, 2012.

[5] F X. Giraldo, J F.. Kelly, and E. Constantinescu. Implicit-explicit formulations of a three-dimensional Nonhydrostatic Unified Model of the Atmosphere (NUMA). *SIAM J. Sci. Comput.*, 35:1162–1194, 2013.

[6] F. X. Giraldo and M. Restelli. A study of spectral element and discontinuous Galerkin methods for the Navier-Stokes equations in nonhydrostatic mesoscale atmospheric modeling: Equation sets and test cases. *J. Comput. Phys.*, 227:3849–3877, 2008.

[7] J L. Guermond and R. Pasquetti. Entropy-based nonlinear viscosity for Fourier approximations of conservation laws. *C. R. Acad. Sci., Ser. I*, 346:801–806, 2008.

[8] G. Houzeaux and J. Principe. A variational subgrid scale model for transient incompressible flows. *International Journal of Computational Fluid Dynamics*, 22:135–152, 2008.

[9] T. Hughes. Multiscale phenomena: Green's functions, the Dirichlet-to-Neumann formulation, subgrid scale models, bubbles and the origins of stabilized methods. *Comput. Methods Appl. Mech. and Engrg.*, 127:387–401, 1995.

[10] T J R Hughes, L P Franca, and G M Hulbert. A new finite element formulation for computational fluid dynamics: III. the Galerkin/least-squares method for advection-diffusive equations. *Comput. Methods Appl. Mech. Eng.*, 73:329–336, 1989.

[11] J. F. Kelly and F. X. Giraldo. Continuous and discontinuous Galerkin methods for a scalable three-dimensional nonhydrostatic atmospheric model: limited-area mode. *J. Comput. Phys.*, 231:7988–8008, 2012.

[12] E. Kessler. On the distribution and continuity of water substance in atmospheric circulation. *Meteorol. Monogr.*, 10:32, 1969.

[13] D. K. Lilly. On the numerical simulation of buoyant convection. *Tellus*, 14:148–172, 1962.

[14] S. Marras, M. Moragues, M R. Vázquez, O. Jorba, and G. Houzeaux. Simulations of moist convection by a variational multiscale stabilized finite element method. *J. Comput. Phys.*, 252:195–218, 2013.

[15] S. Marras, M. Moragues, M R. Vázquez, O. Jorba, and G. Houzeaux. A variational multiscale stabilized finite element method for the solution of the Euler equations of nonhydrostatic stratified flows. *J. Comput. Phys.*, 236:380–407, 2013.

[16] M. Nazarov. Convergence of a residual based artificial viscosity finite element method. *Comput. Math. Appl.*, 65(4):616–626, 2013.

[17] M. Nazarov and J. Hoffman. Residual-based artificial viscosity for simulation of turbulent compressible flow using adaptive finite element methods. *Int. J. Numer. Methods Fluids*, 71:339–357, 2013.

[18] J. Smagorinsky. General circulation experiments with the primitive equations: I. the basic experiement. *Mon. Wea. Rev.*, 91:99–164, 1963.

[19] S. Soong and Y. Ogura. A comparison between axisymmetric abd slab0symmetric cumulus cloud models. *J. Atmos. Sci.*, 30:879–893, 1973.

[20] J. Straka, R. Wilhelmson, L. Wicker, J. Anderson, and K. Droegemeier. Numerical solution of a nonlinear density current: a benchmark solution and comparisons. *Int. J. Num. Meth. in Fluids*, 17:1–22, 1993.